View metadata, citation and similar papers at core.ac.uk

brought to you by CORE

provided by CERN Document Server

UNIVERSITY
of
GLASGOW

D

Telep

Comparison of Dijet Cross Sections vs Q^2 with Various Monte Carlo Models

N. Macdonald[a]

[a] Dept. of Physics and Astronomy,
University of Glasgow, Glasgow, U.K.

Abstract

The dijet cross section as a function of both the fraction of the photon momentum participating in the hard process, x_γ^{OBS}, and the photon's virtuality, Q^2, is compared with the predictions of Herwig 5.9 for various photon parton distribution functions. The ratio of dijet cross sections with $x_\gamma^{OBS} < 0.75$ and $x_\gamma^{OBS} > 0.75$ is measured as a function of Q^2. This ratio is found to decrease as Q^2 increases consistent with the hypothesis that the photon parton distribution functions decrease with increasing photon virtuality.

1 Introduction

Experimental information on the partonic structure of the photon is obtained from the HERA ep collider experiments via measurements of jet photoproduction [1]. Leading order (LO) QCD predicts that photon interactions have a two-component nature. In direct photon processes the entire momentum of the photon takes part in the hard subprocess with a parton from the proton whereas in resolved photon processes, the photon acts as a source of partons and one of these enters the hard subprocess. By tagging inclusive dijet events (two or more jets) in conjunction with tagging the scattered electron, information on the structure of the photon can be extracted as a function of the virtuality of the photon, Q^2.

2 Direct and Resolved Photoproduction

Jet photoproduction events are split into two classes

1. Direct photoproduction. Here the virtual photon connects directly to a quark line in the Feynman diagram, the quark absorbing the photon. The fraction of the photon's four momentum entering the hard dijet subprocess, x_γ^{LO}, is equal to unity.

2. Resolved photoproduction. Here the virtual photon behaves as a source of partons, one of which takes part in the hard subprocess. One of the main signatures of a resolved process is that of the low p_T photon remnant, the partons produced by the photon which did not take part in the scatter. The fraction of the photon's four momentum entering the hard dijet subprocess, x_γ^{LO}, is now less than unity.

An example of each process is shown in figure 1. On the left is an example of the diagram corresponding to a direct process, on the right is an example of a resolved process.

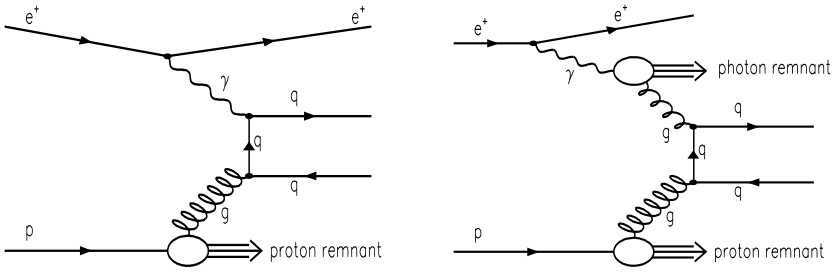

Figure 1: *Feynman diagrams of direct and resolved process*

2.1 $\mathbf{x_\gamma^{obs}}$

Experimentally x_γ^{LO} cannot be measured directly, so the variable x_γ^{obs} is chosen as an estimator of the fraction of the photon's momentum that takes part in the hard scatter. x_γ^{obs} is then the fraction of the photon momentum manifest in the two highest p_T jets and is defined by the equation

$$x_\gamma^{obs} = \frac{\sum_{j=1}^{2} E_{Tj} e^{-\eta_j}}{2E_e y} = \frac{\sum_{j=1}^{2}(E_j - p_{z_j})}{\sum_{hadrons}(E - p_z)}$$

where E_{Tj} is the transverse energy of jet j, η_j is the pseudorapidity of the jet, and y is the inelasticity of the event.

The fact that jets of hadrons are measured, and not partons means that the value of x_γ^{obs} is dependent upon the jet finding algorithm used, and hadronisation effects. Events with a high value of x_γ^{obs} are mostly direct processes, low x_γ^{obs} resolved processes. As a result of this, "direct enriched" events are classed as being those with $x_\gamma^{obs} > 0.75$, and "resolved enriched" events as those with $x_\gamma^{obs} < 0.75$. This is an experimental definition, since there are still true resolved events with $x_\gamma^{obs} > 0.75$, and vice versa, but the contamination between the two event classes is minimised by having the cut at this value.

3 Comparison of Data Cross Sections with Monte Carlo

The cross section that is measured is defined by the following set of kinematic cuts

- Inclusive dijets (k_T clustering algorithm) [2]
- $Q^2 < 1.0$, $0.1 < Q^2 < 0.55$, $1.5 < Q^2 < 4.5$ (GeV^2)
- $0.20 < y < 0.55$
- $E_T^{jets} > 5.5$ GeV
- $-1.125 < \eta^{jets} < 2.2$

Three different Q^2 regions are accessed, firstly $Q^2 < 1.0$ GeV^2 corresponds to quasi-real photons, where the electron is not tagged, and the large bulk of such events lead to a median Q^2 of 0.001 GeV^2. For $0.1 < Q^2 < 0.55$ GeV^2 ZEUS has a small angle electron detector [3, 4] for tagging events in the transition region between photoproduction and DIS. For $1.5 < Q^2 < 4.5$ GeV^2 the electron is tagged in the ZEUS main calorimeter [5].

Figure 3 contains the dijet cross sections shown as a ratio of resolved enriched over direct enriched as a function of Q^2. Since certain systematic errors cancel in the ratio, this is a more precise measurement than absolute differential cross sections. The ratio is also sensitive in shape (but not normalisation) to the photon PDF, even when the absolute cross section given by Herwig 5.9 [6] does not match the data. One can see that GRV LO [7] is flat, as expected, since it has no Q^2 dependence. The effect of multi-parton interactions is to increase the ratio, but again for GRV LO this is flat vs Q^2.

The Lepto 6.5.1 [8] prediction is also flat since this contains direct processes only. Even with direct only processes, the ratio of resolved enriched over direct enriched cross sections is non-zero, demonstrating that x_γ^{obs} is sensitive to the jet finding algorithm and hadronisation effects, and hence has a reduced correlation with x_γ^{LO}. The data is approaching this direct only limit, however resolved processes are still required in order to describe the data up to a Q^2 of 4.5 GeV^2.

The Schuler and Sjöstrand (SaS1D) photon PDF [9] does have a suppresion of parton densities in the photon vs Q^2, and this can be clearly seen from the shape of the curves. The effect of multi-parton interactions is small for this PDF, and both curves approach the data for the higher Q^2 bins, whilst disagreeing for lower Q^2 values. Given the size of the errors on the data, the shape of these curves is consistent with the ZEUS data.

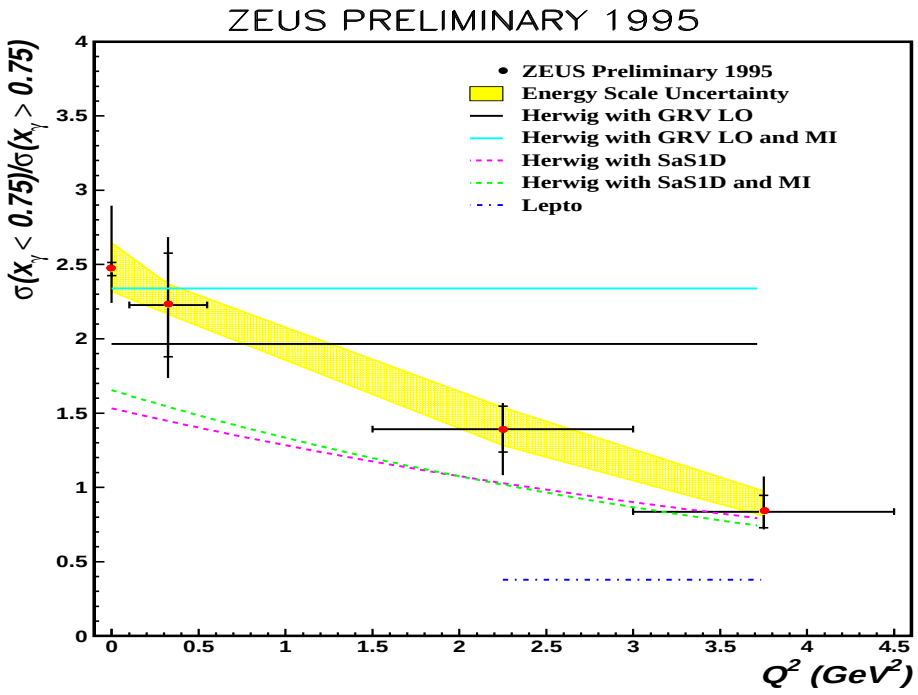

Figure 2: *Ratio of resolved enriched to direct enriched dijet cross sections. Theory curves are produced by Herwig 5.9, with various photon PDFs. Also shown is the result of Lepto 6.5.1*

References

[1] ZEUS Collab., M. Derrick et al., *Phys. Lett.* **B322** (1994) 287;
ZEUS Collab., M. Derrick et al., *Phys. Lett.* **B348** (1995) 665;
ZEUS Collab., J. Breitweg et al., *Eur. Phys. J.* **C1** (1998) 109;
H1 Collab. T. Ahmed et al.,*Phys. Lett.* **B297** (1992) 205;
H1 Collab. I. Abt et al., *Phys. Lett.* **B314** (1993) 436;
H1 Collab. C. Adloff et al., *Eur. Phys. J.* **C1** (1998) 97.

[2] S. Catani, Yu.L. Dokshitzer, M.H. Seymour and B.R. Webber, *Nucl. Phys.* **B406** (1993) 187;
S.D. Ellis and D.E. Soper *Phys. Rev.* **D48** (1993) 3160.

[3] A Nucl. Inst. Meth. paper in preparation on the BPC design and performance.

[4] J.Breitweg et al., *Phys. Lett.* **B407** (1997) 432-448.

[5] M. Derrick et al., *Nucl. Instrum. Methods* **A309** (1991) 77;
A. Andresen et al., *Nucl. Instrum. Methods* **A309** (1991) 101;
A. Bernstein et al., *Nucl. Instrum. Methods* **A336** (1993) 23.

[6] Herwig 5.9; G. Marchesini et al., *Computer Phys. Comm.* **67** (1992) 465.

[7] M. Gluck, E. Reya and A. Vogt, *Phys. Rev.* **D46** (1992) 1973.

[8] G.Ingelman, A. Edin and J. Rathsman, *Computer Phys. Comm.* **101** (1997) 108-134.

[9] G.Schuler and T. Sjöstrand, *Phys. Lett.* **B376** (1996) 193.